NMR Study of Water-Filled Pores in One of the Most Widely Used Polymeric Material: The Paper

D. Capitani,* N. Proietti, F. Ziarelli, and A. L. Segre

Institute of Chemical Methodologies, CNR Area della Ricerca di Roma, M.B.10, 00016 Monterotondo Staz., Roma, Italy

Received February 4, 2002

ABSTRACT: An NMR study of good quality paper is reported. Good quality paper is a polymeric bicomponent material made with cellulose and water plus impurities. Water is located into pores. The removal of even a small amount of the water from paper causes an irreversible destruction of the material. According to the IT method, the intensity of the water resonance as a function of the temperature has been used for obtaining the pore size distribution. A strongly asymmetric distribution with a well-defined maximum at 1.4 nm has been found. The average size of water pools has been confirmed applying NMR techniques suitable for studying spin diffusion processes, i.e., dipolar filtered methods and 2D WISE. Both techniques show that the water pools are surrounded by amorphous cellulose. Crystalline domains surround amorphous domains which in turn include the water pools. Dipolar filtered methods allow a rough evaluation of the distance between crystalline domains, this is, about 3 nm. This distance agrees with a previous result obtained by transmission electron microscopy (TEM) methods. Our results give an insight into the paper morphology. It must be pointed out that a clear description of the paper morphology is important for the restoration and preservation of ancient paper.

Introduction

Paper is one among the most antique man-made material. It is primarily composed by long fibers of cellulose. In low-quality paper, this cellulose embeds in a hemicellulose and lignin matrix. In antique and laboratory prepared high-quality paper, only cellulose fibers are present.[1] Crystalline fibers are present as polymorphs, always in the stable forms[2] of cellulose I_α and I_β. The polymorphic composition reflects the fiber botanical origin.[3] Amorphous cellulose can be as high as ≈40−60%.

Cellulose is not the only primary component. An almost equimolar amount of bound water is always present.[4] Water−cellulose interaction has been studied many years ago using many techniques including moisture sorption, deuterium exchange on the OH groups, and infrared studies of deuterated cellulose.[5] More recently, in NMR studies performed on cellulose, strong water−cellulose interactions were observed.[6] However, in all polymorphous structures,[7] water is not present as a constituent in the crystallites of cellulose. In paper strong spin diffusion is present between cellulose and water;[8] thus, water domains must somehow permeate the cellulose domains.

The purpose of this work is to characterize the water component present in paper and to find a relationship between the structure of the water pools and suitable NMR parameters. Note that in many materials pores dimension can be studied removing the water from the porous system and using solvents or helium or xenon to measure the pore diameter. All these methods are unsuitable in the case of paper since the removal of even a small amount of water results in a permanent destruction of the material.[9] Following a well-established method[10] which correlates the intensity of the water component as a function of the temperature, a pore size distribution was obtained. To verify the distribution function obtained in this way, and for a better understanding of the system morphology, a series of 1D and 2D high-resolution ^{13}C CP-MAS spectra were obtained using dipolar filter and WISE sequences.[11]

Experimental Procedures

^{1}H Pulsed Low-Resolution NMR. ^{1}H pulsed low-resolution NMR experiments were performed on a commercial spectrometer "Spinmaster" of Stelar, Mede (PV) Italy, operating between 10 and 85 MHz. In the temperature range 77−320 K a variable temperature unit (Stelar VTC91) equipped with a standard Bruker nitrogen evaporator system or with a nitrogen flow from a pressurized line was used.

Samples of conditioned Linters paper[4] (23 °C, 50% RH at least 1 week) were finely cut, introduced into standard 5 mm NMR tubes, and then sealed. To keep the paper samples well within the NMR receiver coil, the height of samples was 0.5 cm; the weight of each sample was 25 mg.

The 90° pulse was 3.8 μs, and the dead time of the instrument was 8 μs.

^{1}H T_1 spin−lattice relaxation times were measured at 57 and 81 MHz using the aperiodic saturation recovery (APSR) sequence.[4]

Spin−lattice relaxation times in the rotating frame $T_{1\rho}^{^1H}$ were measured with an effective field $B_1 = 64$ kHz and a carrier frequency 40 MHz. At least 128 spin-lock pulses were used in each experiment.

Intensities relative to the water resonance were collected at 81 MHz in the range 180−300 K, the step being 5 °C.

^{13}C CPMAS-NMR. Samples of conditioned paper (Linters), about 70 mg, were finely cut and packed into 4 mm zirconia rotors and sealed with Kel-F caps. Solid-state ^{13}C CP-MAS NMR spectra were performed at 50.13 MHz on a Bruker AMX-200 spectrometer and at 150.13 MHz on a Bruker Avance 600 spectrometer. In all measurements the spin rate was 5 kHz. The cross-polarization was performed applying a variable spin-lock sequence RAMP−CP-MAS,[20] with a contact time 1 ms and a recycle delay 4 s.

Spectra were obtained using 1024 data points in the time domain, zero-filled and Fourier transformed to a real size of 1024 data points.

$T_{1\rho}^{^1H}$ and $T_{1\rho}^{^{13}C}$ Measurements.[21] ^{1}H and ^{13}C spin−lattice relaxation times in the rotating frame, $T_{1\rho}^{^1H}$ and $T_{1\rho}^{^{13}C}$, were measured on a Bruker Avance 600 NMR spectrometer.

10.1021/ma020174w CCC: $22.00
Published on Web 06/04/2002

The spin−lattice relaxation time in the rotating frame for the abundant spin describes the rate at which a nuclear magnetization, spin-locked in the rotating frame, approaches its thermal equilibrium value.

In the spin-locking process, the magnetization is brought into the $x-y$ plane by a $\pi/2$ pulse, after which the phase of the radio-frequency signal is changed to spin-lock the magnetization on the y axis in the rotating frame. Since the effective magnetic field in the rotating frame B_{eff} is orders of magnitude smaller than B_0, the rotating frame magnetization is much larger than its thermal equilibrium value. Thus, the magnetization decays toward the equilibrium value with the time constant $T_{1\rho}^{^1\text{H}}$.

$T_{1\rho}^{^1\text{H}}$ was measured with an effective field $B_{\text{eff}} = 58$ kHz and with a carrier frequency 600.13 MHz; the variable spin-lock pulse t_i ranged from 0.1 to 25 ms.

$T_{1\rho}^{^{13}\text{C}}$ was measured with an effective field $B_{\text{eff}} = 58$ kHz and with a carrier frequency 150.13 MHz; the variable spin-lock pulse t_i ranged from 0.1 to 35 ms.

The obtained data were fit to the equation

$$y = we^{-t/T_{1\rho}} + C_0$$

where w is the weight of the exponential function, c_0 is the average value of the experimental noise, and $T_{1\rho}$ is the spin−lattice relaxation time in the rotating frame.

In all cases a single-exponential trend was found.

Dipolar Filtered Experiment. A selection between mobile and rigid domains can be performed using a "dipolar filter". The dipolar filter sequence consists of n $\pi/2$ pulses used as a filter with an interpulse delay of p μs used to adjust the filter strength.[22] In our case $n = 12$ and $p = 12$ μs.

Two phase-cycled $\pi/2$ pulses equivalent to alternate 0 and π pulses were used to flip the magnetization to the $(-z)$ axis and eliminate the effects of T_1 relaxation.[23]

The mixing times for these experiments ranged from 0.5 to 6000 ms.

For all selected resonances, the value of $\sqrt{\tau_m^*}$ was obtained according to the initial rate approximation method.[19]

2D-WISE NMR Experiment. The 2D-WISE experiments[24] were performed with a cross-polarization contact time 0.3 ms. The data matrix has a size of 256 data points in the ^{1}H dimension, t_1, and 1024 data points in the ^{13}C dimension, t_2. The t_1 and t_2 dimensions were zero-filled to 2048 and 1024 real data points, respectively; an exponential multiplication was applied in both dimensions, with a line broadening 64 and 128, respectively.

The recycle delay was 3 s. The mixing time spanned from 0.5 to 40 ms.

Results and Discussion

^{1}H NMR: Pore Size Distribution. At temperatures higher than 210 K, the ^{1}H FID of any sample of paper shows always two components (see Figure 1, top). The fast decaying one is due to cellulose, and the slow decaying one is due to water. After a Fourier transformation (see Figure 1, bottom), the cellulose component appears as a broad hump, on top of which a rather sharp resonance due to water can be observed.

In any piece of well preserved conditioned paper the molar ratio[9] between the water component and the cellulose component is about 0.90 ± 0.05.

As previously shown, at room temperature the spin−lattice relaxation time of both components shows a multiexponential behavior.[9] In a solid system like paper in the presence of paramagnetic impurities, spin−lattice relaxation always appears multiexponential.[25] Moreover, the higher the paramagnetic impurities content, the shortest are T_1 values. Thus, it is the proximity to paramagnetic impurities that modulates the T_1 value. Note that in Linters paper the spin density of the longest T_1 component takes into account more than about 90% of the total magnetization.

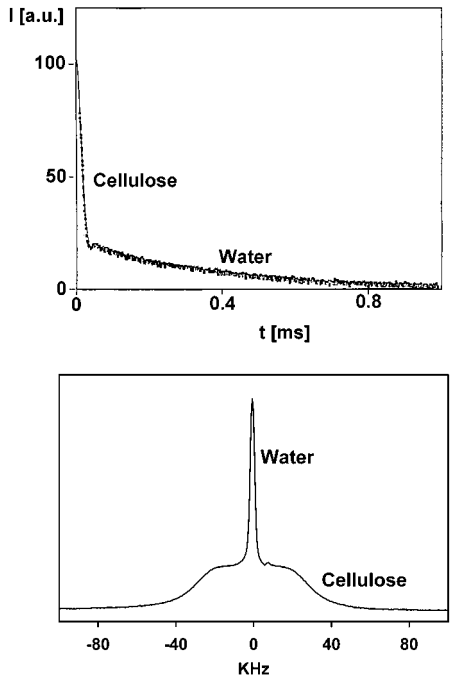

Figure 1. (top) Free induction decay of Linters paper: the fast decaying component is due to cellulose, and the slow decaying component is due to water. (bottom) After applying a Fourier transformation, the proton wide line spectrum is obtained: the broad line is due to cellulose (≈64 kHz wide), and the sharp line is due to water (≈1.5 kHz wide).

In all paper samples, independent of the nature or content of paramagnetic impurities, the longest T_1 components of the water and that of cellulose are always equal within the experimental error. Thus, a strong spin diffusion is present, able to equalize T_1 values. This means that domains either of water or of cellulose must be rather small, and an upper limit can be set. To evaluate this limit, we may use the approach of McBrierty.[26] Considering this simple approach and all T_1 and T_2 data previously obtained in more than 30 different paper samples, an upper limit can be set for the diameter of water pools, which must be lower than a value R in the 4−11 nm range.

Relaxometric studies performed as a function of the temperature confirm this estimate and set a lower limit to very small dimensions. In fact, in paper, "free to move" water has been observed at temperatures as low as about 210 K. Since the lowering of the melting point is associated with a confinement into small cavities or pores,[10−18] we may relate this extreme melting temperature variation to the presence of really small pores. We can then treat the paper as a porous system containing a mobile species, water, embedded into a rigid matrix of cellulose. The physical properties of a liquid confined within small pores are different than the properties of the bulk material; in particular, the melting temperature of the confined liquid is depressed and tightly related the pore size distribution itself.

Conventional methods used in determining pore sizes in porous media are based on gas adsorption−desorption techniques[27] and mercury porosimetry.[28] NMR methods for the determination of pore size are based on Xe or He spectroscopies.[29]

All these methods cannot be applied in the case of paper. In fact, the paper pores are full of water, and

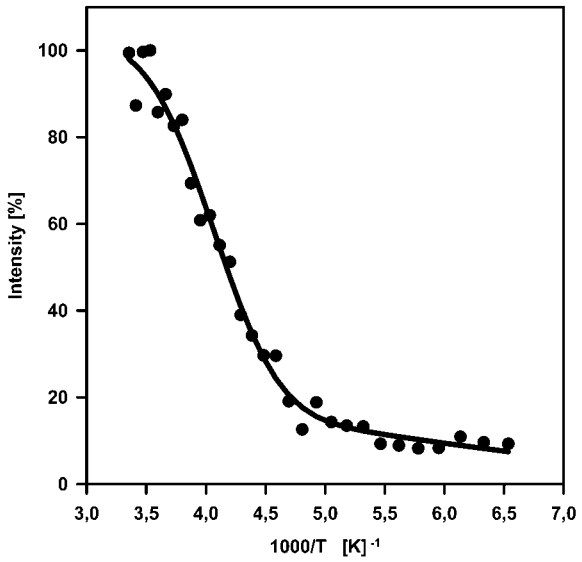

Figure 2. *IT* plot: the normalized intensity of the water resonance is reported as a function of 1000/*T*. By lowering the temperature, the intensity of the water resonance decreases in a slow and continuous way. The line through the experimental points has been obtained fitting the experimental data to eq 1.

the water itself plays a crucial role in stabilizing the paper structure,[9] its removal causing a complete collapse of the paper structure.

It has been shown recently[10−18] that ^{1}H NMR, a nondestructive technique, can be used for characterizing the porous distribution of mesoporous materials. This approach uses the water itself as a probe molecule. Then freezing phenomena of water restricted into small volumes can give information on pore size distribution.

The signal intensity of the water resonance is measured as a function of the temperature. These curves, intensity vs temperature, i.e., *IT* plots, represent a porous network without requiring any model of the shape of the pore itself.

Inorganic materials such as zeolites and other silicate samples[15,16] have been characterized with the *IT* method.

It has been also shown that the *IT* method can be applied in porous systems with a pore size *R* ranging from few tenths of a nanometer up to a few tens of nanometers. The pore size distribution obtained applying the ^{1}H NMR technique compares well with the corresponding distribution obtained with N_2 adsorption measurements.[14]

Thus, this method is suitable for obtaining the pore size distribution in paper.

At 300 K, the ^{1}H wide line spectrum of paper shows two superimposed resonances (see Figure 1, bottom), with a line width about 64 kHz and about 1.5 kHz.

By lowering the temperature, the water resonance progressively broadens and loses intensity; finally, at ∼200 K it fully disappears into the broad cellulose resonance.

According to the *IT* method, the intensity of the water resonance has been reported as a function of 1000/*T* (see Figure 2). By lowering the temperature, the intensity of the water resonance decreases in a slow and continuous way.

These data have been used for obtaining physical parameters related to the water mobility.

As a function of $X = 1000/T$, the intensity of the water resonance can be written as

$$I(X) = \sum_{i=1}^{N} \frac{I_{0i}}{\sqrt{\pi}} \int_0^{(X-X_C)/\Delta_i\sqrt{\pi}} \exp(-u^2)\, du$$

$$\text{equivalent to} \quad I(X) = \sum_{i=1}^{N} \frac{I_{0i}}{2}\left[1 + \operatorname{erf}\left[\frac{X_c - X}{\Delta_i\sqrt{2}}\right]\right] \quad (1)$$

This expression has been obtained by applying known models for molecular motion in fluids and solids,[11] leading to a log-normal distribution $P(\tau)$:

$$I(X) = \int_0^{\tau_C} P(\tau)\, d\tau$$

$I(X)$ represents the amount of mobile pore water at the inverse temperature $X = 1000/T$, I_{0i} is the amount of confined pore water, $X_{ci} = 1000/T_{ci}$ with T_{ci} being the phase transition temperature, and Δ_i is the width of the transition curve. Note that, for a sharp transition, the Δ_i value tends to 0, while the broader the transition, the higher is the Δ_i value. Moreover, the higher the X_{ci} value, the smaller the pore size. Finally, N in (1) is the number of the temperature transitions.

Parameters I_0, X_c, and Δ were obtained fitting the experimental data shown in Figure 2 to eq 1. In our case $N = 1$.

The solid line through the experimental points was obtained applying the best fit procedure (see Figure 2).

Differentiating eq 1 with respect to X, the melting points distribution curve is obtained:

$$\frac{dI}{dX} = \sum_{i=1}^{N} \frac{I_{0i}}{\sqrt{2\pi}\Delta_i} \exp\left[-\left(\frac{X - X_{ci}}{\sqrt{2}\Delta_i}\right)^2\right] \quad (2)$$

This distribution curve is a simple sum of Gaussian functions centered at X_{ci} with half-width Δ_i.

The following relationship can be used:

$$\frac{dI}{dR} = \frac{dI}{dX}\frac{dX}{dR} \quad (3)$$

An equation has been derived which correlates the freezing point temperature depression ΔT of the confined water to the pore radius R:

$$\Delta T = \frac{K_f}{R + t_f} \quad (4)$$

where $\Delta T = T_0 - T_c$; $T_0 = 273.15$ K is the freezing temperature of the free water.

According to the literature,[14] the values of parameters t_f and K_f have been obtained fitting the model eq 4 to the experimental data obtained for several samples. Hence, the obtained values should be acceptable for a general case. It has been also shown[14] that at sufficiently large pore radius, $R \gg 0.35$ nm, the size of the nonfreezing surface layer t_f is much smaller than the pore radius, and eq 4 can be approximated with the Gibbs and Thomas equation, i.e.

$$\Delta T = K_f/R, \quad K_f = 676 \text{ K Å}^{-1}$$

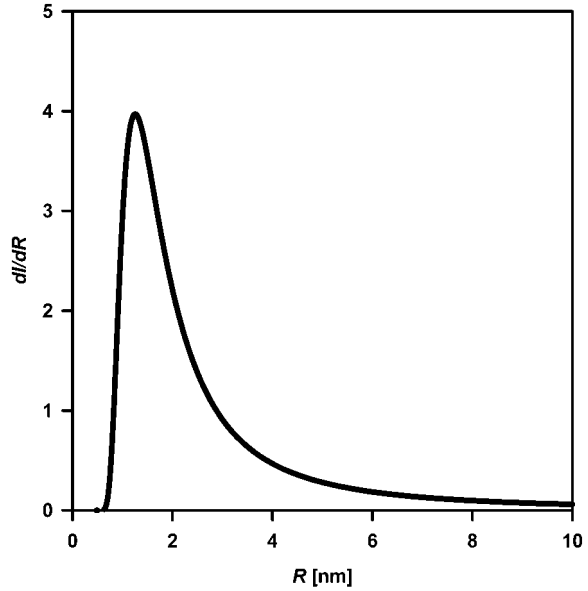

Figure 3. Pore size distribution of Linters paper: note the asymmetric distribution with a well-defined maximum at 1.4 nm.

From eq 4

$$X = \frac{1000(t_f + R)}{(T_0R + T_0t_f - K_f)^2} \tag{5}$$

The derivative of eq 5 on respect X is

$$\frac{dX}{dR} = \frac{1000K_f}{(T_0R + K_f)^2} \tag{6}$$

Substituting (2) and (6) into (3), the pore size distribution curve is obtained:

$$\frac{dI}{dR} = \sum_{i=1}^{N} \frac{I_{0i}}{1000K_f\Delta_i\sqrt{2\pi}}(XT_0 - 1000)^2 \exp\left[\frac{-(X - X_{ci})^2}{\Delta_i\sqrt{2\pi}}\right] \tag{7}$$

The analytical expression obtained from paper experimental data applied to (7) and (1) leads to $X_c = 4.066$, $\Delta = 0.47$, and $I_0 = 100$. The corresponding pore size distribution is shown in Figure 3.

The distribution shows a maximum at $R = 1.4$ nm. The distribution is asymmetric, abruptly decreasing for values $R_i < 1.4$ nm and decreasing smoothly for values $R_i > 1.4$ nm.

Low-Resolution $T_{1\rho}(^1H)$ Measurements. At 300 K on the water resonance, two different $T_{1\rho}$ components can be measured; their value is $T_{1\rho} = 1.8 \pm 0.2$ ms and $T_{1\rho} = 11 \pm 3$ ms, while for the cellulose resonance only one value can be measured, $T_{1\rho} = 12 \pm 2$ ms. In Whatman paper (free of paramagnetic impurities and sizing) the water component shows slightly longer values, $T_{1\rho} = 2.2 \pm 0.2$ ms and $T_{1\rho} = 21 \pm 4$ ms, while for the cellulose component $T_{1\rho} = 15 \pm 3$ ms. All these data point to a large distribution of pore size with a set of pores unable to give spin diffusion on a $T_{1\rho}$ scale, while for other pores the spin diffusion process is fully operative even on a $T_{1\rho}$ scale.

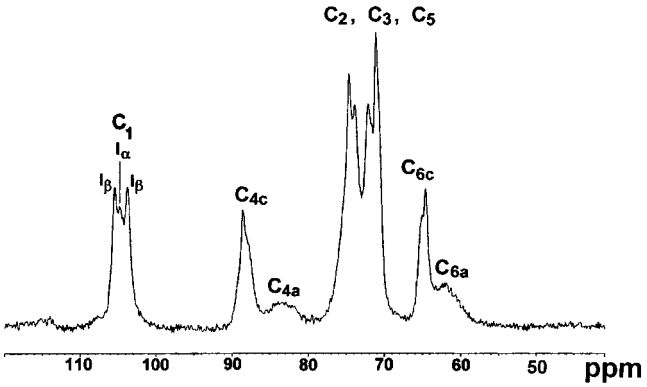

Figure 4. ^{13}C CP-MAS NMR spectrum at 150.13 MHz of Linters paper. Chemical shift values and the full assignment are reported in Table 1.

^{13}C NMR Measurements in MAS Conditions. All previously reported data rely on several hypothesis and on values obtained on inorganic porous systems. To verify the *IT* results, different approaches were attempted all based on CP-MAS ^{13}C NMR spectroscopy.

The CP-MAS spectrum of paper performed at 150.13 MHz is reported in Figure 4. On the resonance at ≈106 ppm due to the anomeric C atom the presence of the two crystalline polymorphous forms, I_α and I_β, is pointed out.[2] Resonances labeled with a "c" are due to the crystalline domains (I_α and I_β), while the broad resonances labeled with an "a" at 85.4 and 64.5 ppm are respectively due to C_4 and C_6 of cellulose in an amorphous environment. Note that the NMR spectrum of a fully random cellulose from algae is completely different from the spectrum of the amorphous component of cellulose in paper.[3] In agreement with the literature,[30] we can hypothesize that amorphous cellulose in paper is present in an extended form, exactly like crystalline cellulose.[7] However, the regular net of H bonds which holds together crystalline cellulose is fully altered in the amorphous domains.[30] Thus, we can think of two amorphous environments: one due to cellulose interconnecting I_α and I_β domains and another one surrounding the water pools.

To confirm the efficiency of the cross-polarization transfer for crystalline and for amorphous domains, a CP-MAS spectrum at 260 K was performed and compared with the spectrum obtained at 300 K. The crystalline/amorphous ratio measured in both experiments does not change.

$T_{1\rho}(^1H)$ and $T_{1\rho}(^{13}C)$. $T_{1\rho}(^1H)$ is different from $T_{1\rho}(^{13}C)$ in that $T_{1\rho}(^1H)$ is sensitive to the motion of the ^1H system averaged by spin diffusion over a short distance while $T_{1\rho}(^{13}C)$ reflects the motion of individual ^{13}C spins.[21] Thus, the ^1H relaxation is sensitive to macroscopic variations while the ^{13}C relaxation is site specific. All data relative to both parameters are given in Table 1.

A possible interpretation of the experimental results needs the observation that some ^{13}C resonance is entirely due to the amorphous part of the material, while some other is entirely due to the crystalline fraction and other resonances are due to both (see Figure 4).

All $T_{1\rho}(^{13}C)$ values due to methines are equal within the experimental error. Thus, the same local motions contribute to the observed values, and these motions are

Table 1. Chemical Shifts and Relative Assignment of ^{13}C Resonances in Paper[a]

δ (ppm)[b]	$T_{1\rho}(^1H)$ (ms)	$T_{1\rho}(^{13}C)$ (ms)
C_1 106.3	11.3 ± 0.7	6.8 ± 0.5
C_{4c} 90.3	15.8 ± 0.6	6.7 ± 0.4
C_{4a} 85.4	6.8 ± 0.5	8 ± 1
$C_{2,3,5}$ 76.4	9.6 ± 0.7	7.0 ± 0.4
$C_{2,3,5}$ 72.9	13.8 ± 0.9	8.0 ± 0.5
C_{6c} 66.8	15 ± 1	2.0 ± 0.1
C_{6a} 64.5	8 ± 1	2.3 ± 0.1

[a] $T_{1\rho}(^1H)$ and $T_{1\rho}(^{13}C)$ values for all carbon resonances; the effective field was 54 kHz [b] Chemical shifts are measured with linear polyethylene as internal standard; the resonance of crystalline polyethylene is taken at 33.63 ppm with respect to tetramethylsilane at 0.0 ppm.

more or less the same both for the crystalline and for the amorphous domains. On the contrary, $T_{1\rho}(^{13}C)$ of methylenes are much shorter, but again the same value is measured on both crystalline and amorphous domain. According to literature data on the extended nature of cellulose chains,[30] both in the amorphous and in the crystalline domains, we observe the same type of local motions for all chains regardless of their environment. Obviously, because of the ω torsion angle, a major degree of freedom is observed on methylenes.

^1H spin−lattice relaxation in the rotating frame, $T_{1\rho}$, was measured directly on each ^{13}C resonance (see Table 1). On those resonances entirely due to the crystalline fraction a rather long $T_{1\rho}(^1H)$ value is measured. This value is quite well comparable with the $T_{1\rho}(^1H)$ value measured directly by ^1H relaxometric methods on the cellulose component. $T_{1\rho}(^1H)$ shows a value intermediate between the two components of $T_{1\rho}(^1H)$ measured on the water component using pulse low-resolution methods. Thus, we can reasonably make the hypothesis that spin diffusion from the water signal operates differently on the amorphous and on the crystalline fractions. Therefore, the water pools are confined by amorphous domains; i.e., water pools do not touch at all crystalline domains.

Dipolar-Filtered ^1H Spin Diffusion Observed through ^{13}C Resonances. As previously shown, the proton wide line spectrum of paper shows a rather sharp resonance due to the water and a broad resonance due to the cellulose. Their line widths at half-height are about 1.5 and 64 kHz, respectively. Since the line width of an ^1H wide line spectrum characterizes the strength of the dipolar coupling among protons and therefore the molecular mobility, this marked difference in the line width values allows the use of the dipolar filter technique.[19] This technique has been previously applied for investigating the spatial separation between regions with mobile and rigid side chains in polymers,[22] for studying the microphase structure in block copolymers,[23] for investigating phase-separated polymer systems,[31] and recently in the study of heterogeneous biopolymer mixtures.[32]

In a current model of paper morphology,[33] water pools exist, embedded in a rigid cellulosic matrix. The question arises of the water pools proximity to the crystalline or to the amorphous polymeric domains. The question can be answered by applying the dipolar filter sequence. In this experiment, by applying a dipolar filter, the selection of the magnetization of the mobile component is achieved. As a consequence, at very short mixing times τ, the carbon signals corresponding to the broad ^1H component are filtered. In turn, at long mixing times, when spin diffusion is complete, the conventional ^{13}C CP-MAS spectrum is obtained.

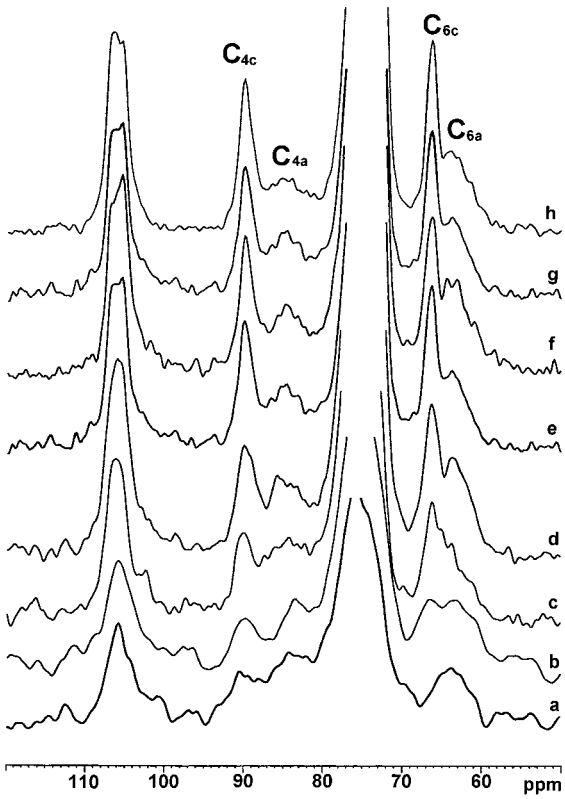

Figure 5. Dipolar filtered ^{13}C CP-MAS NMR spectra of Linters paper at different mixing times τ_i: (a) $\tau_a = 0.5$ ms, (b) $\tau_b = 1$ ms, (c) $\tau_c = 2$ ms, (d) $\tau_d = 3$ ms, (e) $\tau_e = 5$ ms, (f) $\tau_f = 10$ ms, (g) $\tau_g = 20$ ms, and (h) $\tau_h = 40$ ms.

Let us consider the ^{13}C CP-MAS spectrum of paper (see Figure 4). As is well-known,[34] the resonances at 90.3 and 66.8 ppm are respectively due to C_4 and C_6 in a crystalline environment (C_{4c}, C_{6c}) while resonances at 85.4 and 64.5 ppm are due to C_4 and C_6 in an amorphous environment (C_{4a}, C_{6a}). Therefore, at very short mixing time, we should be able to select mostly the carbon resonances belonging to the environment which is closer to the water pools.

Figure 5 shows the dipolar filtered ^{13}C spectra obtained at increasing mixing times. Note that at $\tau = 500$ μs the resonance at 66.8 ppm due to C_{6c} fully disappears, while the resonance at 64.5 ppm due to C_{6a} is still well observable; moreover, the resonance at 85.4 ppm due to C_{4a} is well observable while the intensity of the resonance at 90.3 due to C_{4c} is very low (see Figure 5a). Increasing the mixing time, the intensity of the resonances due to C_{6c} and C_{4c} continuously increases. At τ = 40 ms when the spin diffusion is complete, the normal ^{13}C CP-MAS spectrum is obtained, with the intensity of C_{4c} and C_{6c} resonances very strong on respect to the resonances of their amorphous counterpart (see Figure 5h).

Hence, at very short mixing times, allowing a polarization transfer from the ^1H signal of the water pool to the ^{13}C of the cellulose pool, an indirect selection of the amorphous domain in the cellulose matrix has been performed. Thus, we can hypothesize a model in which a water pool is surrounded by amorphous cellulose layers**.** This model is in agreement with the one suggested by $T_{1\rho}(^1H)$ measurements.

The intensity of the resonances due to C_{4c} and C_{6c} can be reported vs the square root of the mixing time. This

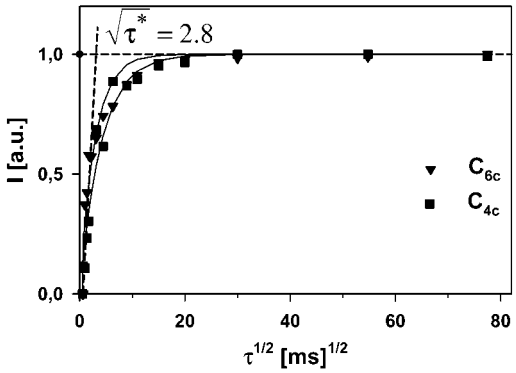

Figure 6. Intensity of C_{4c} and C_{6c} resonances is reported as a function of the square root of the mixing time. The extrapolated value is $\sqrt{\tau^*_m} = 2.8$ ms$^{1/2}$.

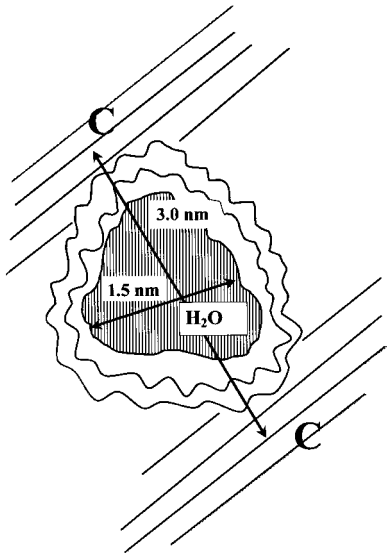

Figure 7. Schematic representation of paper morphology: water pools with an average diameter ≈1.5 nm are surrounded by amorphous cellulose domains. The average distance between two crystalline domains enclosing a water pool is ≈3 nm.

procedure allows the measurement of $\sqrt{\tau^*}$ (see Figure 6). As shown in the figure, $\sqrt{\tau^*}$ is the time at which the initial linear buildup intersects with the extrapolation at long mixing time; $\sqrt{\tau^*} \cong 2.8$ ms$^{1/2}$. The distance R between crystalline domains, including a water pool, can be estimated from the above data (see Figure 7); $R \cong 3$ nm. A full discussion of the approximations used for calculating the distance R will be given in the next paragraph.

Corresponding data on the C_{4c} resonance are less clean. Even at 0.5 ms contact time the resonance at ≈88.8 ppm does not fully disappear, with a very weak broad resonance contributing to the intensity and well observable only at very short contact time (see the trace of Figure 5a with 0.5 ms mixing time). However, omitting this small component, a proper value of the intensity can be read even on the C_{4c} resonance. A plot correlating its intensity to the square root of the mixing time is then obtained (see Figure 6); this plot, even if more noisy, is almost identical to the corresponding one obtained using the C_{6c} resonance. Then the distance R measured from C_{4c} is again of the order of ≈3 nm.

The presence of the very weak broad resonance at ≈88.8 ppm, observed with the dipolar filter at very short mixing time, deserves some comment. A possibility is that there is some chemical shift sensitivity of the C_{4a} resonance to the chemical environment, water or cellulose, or it might be due to the presence of different amorphous environments as it occurs in other polymorphous polymers.[35]

2D WISE. Originally developed by Spiess at al.,[19] the WISE NMR experiment displays, for every resolved carbon resonance, a proton wide-line spectrum which reflects the size of the dipolar coupling of the protons in the proximity of the respective carbon nuclei. Thus, the wide-line ^{1}H NMR spectrum, fully overlapped in the conventional one-dimensional ^{1}H spectrum, can be spread out according to the chemical shifts of the corresponding carbon nuclei. In separating proton wide-line spectra for different ^{13}C resonances, the WISE experiment establishes a correlation between the chemical structure and the molecular mobility. With the insertion of a mixing time period allowing the spin-diffusion among different proton spin pools, WISE NMR can provide information on the domain size ranging from about 0.5 up to 20 nm. Note that the effect of spin diffusion on the ^{1}H magnetization is detected through the amplitude modulation of the carbon resonances generated by cross-polarization.

This technique has been widely applied for characterizing synthetic copolymers and blends in the solid state[6,22−24,31,36] and for characterizing the dynamic behavior in biopolymers.[32]

Given the extreme difference in mobility between water and cellulose, we can use the WISE experiment for studying the water−cellulose interaction in paper.

In Figure 8a the 2D WISE map without any mixing time is shown. In Figure 8b the 2D WISE map with a very short mixing time ($\tau_m = 0.5$ ms) is shown. In the ^{1}H projection only the broad cellulose component is present, corresponding in the ^{13}C domain to all carbon resonances. The absence of the narrow water line points out that the heteronuclear dipolar interaction between the mobile water protons and the carbon resonance of cellulose is missing when the mixing time is extremely short. Hence, at this very short mixing time, the distance between the water protons and ^{13}C nuclei of the polymeric matrix is too large for observing the water resonance. As a consequence, only by lengthening the time during which the spin diffusion process operates, the dynamic information is transferred from the water protons to the ^{13}C nuclei. At longer mixing time, $\tau_m =$ 20 ms; i.e., in the full spin diffusion regime, the narrow line will appear in ^{1}H projection of the WISE map as shown in Figure 8c. 2D WISE experiments were performed at different mixing time, namely, $\tau_m = 0.5$, 1, 2, 3, 5, 12, 20, and 40 ms. In Figure 9 we report the measurement of the buildup of the intensity of the water resonance from the ^{1}H projection corresponding in the ^{13}C dimension to the resonances due to C_{6c} (▼) and C_{6a} (●). Hence, the buildup of the intensity of the water resonance, seen by crystalline and amorphous cellulose domains, leads to the space relationship between these domains and the water pool.[19]

As shown in the figure, the buildup of the water resonance was complete after $\sqrt{\tau^*} = 1.3$ ms$^{1/2}$ for the C_{6a} resonances while $\sqrt{\tau^*} = 2.3$ ms$^{1/2}$ for the C_{6c} resonance.

Note that from the corresponding buildup curve, resulting from the dipolar filtered experiment (see Figure 6), a $\sqrt{\tau^*} = 2.8$ ms$^{1/2}$ was obtained. Since the

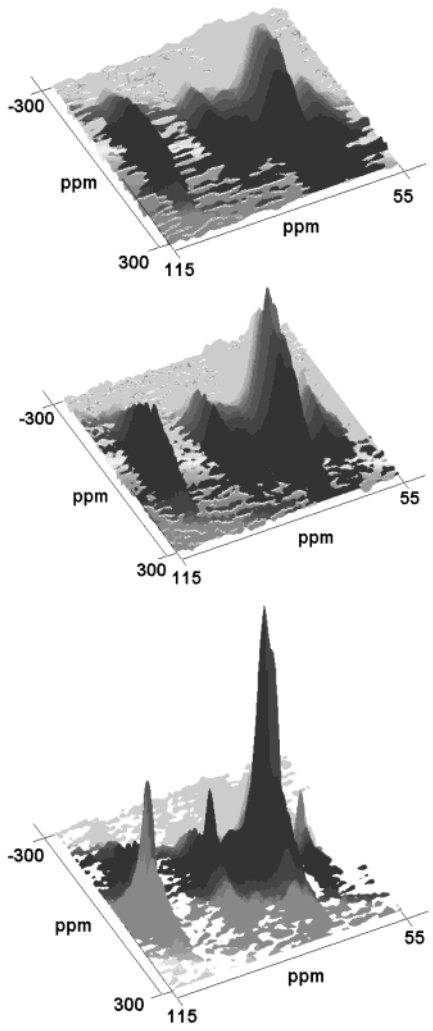

Figure 8. 2D-WISE maps of Linters paper: (a) 2D map without any mixing time before the cross-polarization; (b) 2D map obtained with a very short mixing time, 0.5 ms; (c) 2D map obtained with a long mixing time, 20 ms.

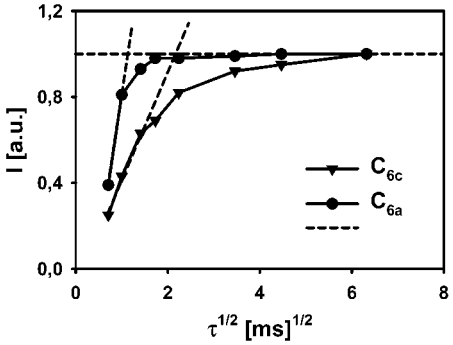

Figure 9. 2D-WISE. The buildup of the water resonance obtained from the ^{1}H projection corresponding in the ^{13}C dimension to the resonances C_{6a} and C_{6c}. The extrapolated values are $\sqrt{\tau^*_m} = 1.3$ and 2.3 ms$^{1/2}$, respectively.

obtained values are in a substantial agreement, we can define an average value $\sqrt{\tau^*} = 2.65$ ms$^{1/2}$, from which the distance $R \cong 3$ nm is obtained; R is the average distance between two crystalline domains including a water pool. Details of this calculation will be given in the next paragraph.

The curve of Figure 9, relative to the amorphous domain, shows that the magnetization of the water resonance spin diffuses to the amorphous cellulose domain in about $\sqrt{\tau^*} = 1.3$ ms$^{1/2}$, while for a magnetization transfer of the water resonance to the crystalline domain $\sqrt{\tau^*} = 2.3$ ms$^{1/2}$.

The above data confirm that the water pool is surrounded by domains of amorphous cellulose.

Water Pools Dimension. Water pool dimensions can be calculated from the data obtained in the WISE and dipolar filtered experiments. Calculation has been performed according to the theory developed by Spiess et al.[37] and previously applied in heterogeneous polymers and blends.

According to this model, we consider a finite source region A, i.e., the water pools, within a finite sink region B, i.e., the cellulose matrix, which is embedded in an infinite matrix consisting of a stoiochiometric mixture of both phases A + B, i.e., water pools + cellulose. In this model the water pools constitute the phase dispersed into the rigid cellulose matrix.

The average size of the dispersed domains (water pools) can be determined knowing the proton density of each phase, the volume fraction of each phase, the volume fraction of the dispersed phase, the diffusivity of each phase, the dimensionality ϵ, and finally the square root of the time τ^*_m in which the magnetization of the dispersed phase (i.e., the water pools) is transferred to the rigid phase (i.e., amorphous cellulose domains) in a spin diffusion regime.

$$d^{\epsilon}_{H_2O} = \left(\frac{\rho^{H}_{H_2O}\Phi_{H_2O} + \rho^{H}_{cell}\Phi_{cell}}{\Phi_{H_2O}\Phi_{cell}}\right)\frac{4\epsilon\Phi_{H_2O}\sqrt{D_{H_2O}D_{cell}}}{\sqrt{\pi}(\sqrt{D_{H_2O}}\rho^{H}_{H_2O} + \sqrt{D_{cell}}\rho^{H}_{cell})}\sqrt{\tau_m}^* \quad (8)$$

The diffusivity of the confined water has been estimated according to literature data,[38,39] $D_{H_2O} \cong 2r_0^2/T_2 = 0.055$ nm^2 ms^{-1}, r_0 being the proton van der Waals radius and $T_2 = 0.5$ ms.

The cellulose diffusivity is proportional to the strength of the dipolar couplings and to the square of the average distance among nearest protons r_{HH}.[37] The strength of the dipolar coupling is proportional to the full width at half-height $\Delta\nu_{1/2}$, which in our case is about 64 kHz, and a typical r_{HH} value for polymers[19] is $r_{HH} \cong 0.25$ nm. Thus, the cellulose diffusivity is $D_{cell} \cong 1.27$ nm^2 ms^{-1}.

The proton density of the water is $\rho^{H}_{H_2O} = \rho_{H_2O}\phi^{H}_{H_2O} = (0.11) \times 10^{-21}$ g nm^{-3}, where $\rho_{H_2O} = 1$ g cm^{-3} is the water density and $\phi^{H}_{H_2O} = 0.11$ g cm^{-3} is the water proton fraction.

The cellulose proton density is $\rho^{H}_{cell} = \rho_{cell}\phi^{H}_{cell} = (0.036) \times 10^{-21}$ g nm^{-3} being $\rho_{cell} = 0.6$ g cm^{-3} and $\phi^{H}_{cell} = 0.06$ g cm^{-3} the cellulose density and the cellulose proton fraction, respectively.

The molar volume fractions are $\Phi_{H_2O} = 0.063$ and $\Phi_{cell} = 0.938$.

ϵ is defined as the number of orthogonal directions relevant for the diffusion process (lamellae: $\epsilon = 1$, cylinders: $\epsilon = 2$, spheres; and cubes: $\epsilon = 3$); in this case $\epsilon = 3$ was assumed.

The $\sqrt{\tau^*_m}$ value relevant for the dimension of the water pools is $\sqrt{\tau^*_m} = 1.3$ ms.

Using all these values, the average diameter of the water pools is $d_{H_2O} \cong 1.5$ nm. Note that the obtained value is in a good agreement with the corresponding value, 1.4 nm, obtained applying the *IT* plot.

The distance R between two crystalline domains including a water pool was performed in the same way using the value $\sqrt{\tau_m^*} = 2.3\ ms^{1/2}$.

Conclusion

Paper is a cellulosic material containing a large quantity of water. In well-preserved good-quality dry paper, an almost equimolar amount of water and cellulose is always present. Water however does not enter into the cellulose matrix and is fully confined into pores. The size and size distribution of these pores filled with water were obtained using *IT* plots; i.e., the intensity of the water resonance was measured as a function of the temperature. From a suitable treatment of the melting temperature of the confined water a strongly asymmetric size distribution of pores was obtained with a well-defined maximum at about 1.4 nm.

The same problem was tackled using two different methods: dipolar filtered ^{13}C CP-MAS spectra and WISE 2D $^{1}H-^{13}C$ map. Both these methods measure the distance between a mobile and a rigid phase using spin diffusion for establishing the space connection between the two phases. Both methods show that water pools are surrounded by amorphous cellulose. In agreement with the dimension obtained with the *IT* plot, the average dimension of water pools is about 1.5 nm.

Moreover, from the dipolar filtered method it is possible to give a rough evaluation of the distance between two crystalline domains which include a water pool; this distance result of the order of 3 nm. This result agrees surprisingly well with previous data obtained from transmission electron microscopy[40] in which the internal diameter of the crystalline core results of the order of 3 nm.

Then, the resulting morphology of paper includes a large number of small water pools in which hydrogen bonds contribute to held together microdomains of amorphous cellulose.

The two used procedures, the *IT* method and WISE and dipolar filtered ^{13}C spectra, even if both relying on NMR measurements, are fully different and independent. The *IT* method is easy, both experimentally as well as for the theoretical calculations involved for obtaining the average dimensions of the water pools and its distribution. However, the *IT* method relies on the melting point of water which is affected by the impurity content. Moreover, the *IT* method does not give any information about the type of cellulose surrounding a water pool.

This information, relevant to the morphology of the system, can be obtained only from ^{13}C spectra obtained in the presence of a dipolar filter or with the WISE 2D map.

Our results give an insight into the paper morphology. It must be pointed out that a clear description of the paper morphology is important for the restoration and preservation of ancient paper.

Acknowledgment. This work was supported by Special ad hoc Project "Cultural Heritage" of CNR and by an EUREKA-EUROCARE project Σ!2214. We thank A. Guarino for continuous support and encouragement.

References and Notes

(1) Roberts, G. A. F. In *Paper Chemistry*; Roberts, J. C., Ed.; Chapman Hall: Glasgow, U.K., 1991; p 9.
(2) Atalla, R. H.; VanderHart, D. L. *Science* **1984**, *17*, 283. Sugiyama, J. J.; Vuong, R.; Chanzy, H. *Macromolecules* **1991**, *24*, 4168.
(3) Torri, G.; Sozzani, P.; Focher, B. In *From Molecular Materials to Solids*; Morazzoni, F., Ed.; Polo Ed. Chimico: Milan, 1993; Chapter 5.
(4) Capitani, D.; Segre, A. L.; Attanasio, D.; Blicharska, B.; Focher, B.; Capretti, G. *Tappi J.* **1996**, *79*, 113.
(5) Jeffries, R. J. *J. Appl. Polym. Sci.* **1964**, *8*, 1213. Knight, J. A.; Lamar Hicks, H.; Stephaens, K. W. *Textile Res. J.* **1969**, *4*, 324.
(6) Radloff, D.; Boeffel, C.; Spiess, H. W. *Macromolecules* **1996**, *29*, 1528.
(7) Chanzy, H.; Herissat, B. *FEBS Lett.* **1985**, *184*, 324. Kroon-Batenburg, L. M. J.; Kroon, J. *Carbohydr. Eur.* **1995**, *12*, 15.
(8) Paci, M.; Federici, C.; Capitani, D.; Perenze, N.; Segre, A. L. *Carbohydr. Polym.* **1995**, *26*, 289.
(9) Attanasio, D.; Capitani, D.; Federici, C.; Paci, M.; Segre, A. L. *ACS Symp. Ser.* **1995**, *598*, 334.
(10) Strange, J. H.; Rahman, M.; Smith, E. G. *Phys. Rev. Lett.* **1993**, *71*, 3589.
(11) Overloop, K.; Van Gerven, L. *J. Magn. Reson.* **1993**, *A101*, 179.
(12) Akporiaye, D.; Hansen, E. W.; Schmidt, R.; Stöcker, M. *J. Phys. Chem.* **1994**, *98*, 1926.
(13) Hansen, E. W.; Schmidt, R.; Stöcker, M.; Akporiaye, D. *J. Phys. Chem.* **1995**, *99*, 4148.
(14) Schimdt, R.; Hansen, E. W.; Stöcker, M.; Akporiaye, D.; Ellestad, O. H. *J. Am. Chem. Soc.* **1995**, *117*, 4049.
(15) Hansen, E. W.; Stöcker, M.; Schmidt, R. *J. Phys. Chem.* **1996**, *100*, 2195.
(16) Hansen, E. W.; Schmidt, R.; Stöcker, M. *J. Phys. Chem.* **1996**, *100*, 11396.
(17) Allen, S. G.; Stephenson, P. C. L.; Strange, J. H *J. Chem. Phys.* **1997**, *106*, 7802.
(18) Hansen, E. W.; Tangstad, E.; Myrvold, E.; Myrstad, T. *J. Phys. Chem. B* **1997**, *101*, 10709.
(19) Schmidt-Rohr, K.; Spiess, H. W. *Multidimensional Solid State NMR and Polymers*; Academic Press: London, 1994.
(20) Metz, G.; Wu, X.; Smith, S. O. *J. Magn. Reson. A* **1994**, *110*, 219.
(21) Stejskal, E. O.; Memory J. D. *High-Resolution NMR in the Solid State*; Oxford University Press: New York, 1994; p 22.
(22) Clauss, J.; Schmidt-Rohr, K.; Adam, A.; Boeffel, C.; Spiess, H. W. *Macromolecules* **1992**, *25*, 5208.
(23) Cai, W. Z.; Schmidt-Rohr, K.; Egger, N.; Gerharz, B.; Spiess, H. W. *Polymer* **1993**, *34*, 267.
(24) Schmidt-Rohr, K.; Clauss, J.; Spiess, H. W. *Macromolecules* **1992**, *25*, 3273.
(25) Bloembergen, N. *Physica* **1954**, *20*, 1130.
(26) McBrierty V. J. Packer,K. J. *Nuclear Magnetic Resonance of Solid Polymers*; Cambridge University Press: New York, 1993; Chapter 6.
(27) Sing, K. S.; Everett, D. H.; Haul, R. A. W.; Moscou, L.; Pierotti, R. A.; Rouquérol, J.; Siemieniewska, T. *Pure Appl. Chem.* **1985**, *57*, 603.
(28) Gregg, S. J.; Sing, K. S. W. *Adsorption, Surface Area and Porosity*, 2nd ed.; Academic Press: New York, 1982.
(29) Watson, A. T.; Philip Chang, C. T. *Prog. NMR Spectrosc.* **1997**, *31*, 343.
(30) Wiley. J. H.; Atalla, R. H. *The Structure of Cellulose*; ACS Symposium Series 340; Atalla, R. H., Ed.; American Chemical Society: Washington, DC, 1987.
(31) Cho, G.; Natansohn, A. *Can. J. Chem.* **1994**, *72*, 2255.
(32) Yan, B.; Stark, R. E. *Macromolecules* **1998**, *31*, 2600.
(33) Heiner, A. P.; Telemann, O. In *Carbohydrases from Trichoderma reesei and other microorganisms: Substrates and industrial Applications*; Claeyssens, M., Nerinckx, W., Piens, K., Eds.; The Royal Society of Chemistry: London, 1998; p 204.
(34) VanderHart, D. L.; Atalla, R. H. *Macromolecules* **1984**, *17*, 1465.
(35) Capitani, D.; Segre, A. L.; Blicharski, J. *Macromolecules* **1995**, *28*, 1121.
(36) Tao, H. J.; Rice, D. M.; MacKnight, J.; Hsu S. L. *Macromolecules* **1995**, *28*, 4036.
(37) Clauss, J.; Schmidt-Rohr, K.; Spiess, H. W. *Acta Polym.* **1993**, *44*, 1.
(38) Bovey, F. A.; Mirau, P. A. *NMR of Polymers;* Academic Press: New York, 1996.
(39) Spiegel, S.; Schmidt-Rohr, K.; Boeffel, C.; Spiess, H. W. *Polym. Commun.* **1993**, *34*, 4566.
(40) Dinand, E.; Chanzy, H.; Vignon, M. R. *Cellulose* **1996**, *3*, 183.

MA020174W